Determining the Short-Range Spin Correlations in the Spin-Chain Li_2CuO_2 and $CuGeO_3$ Compounds Using Resonant Inelastic X-Ray Scattering

Claude Monney,[1] Valentina Bisogni,[1,2] Ke-Jin Zhou,[1] Roberto Kraus,[2] Vladimir N. Strocov,[1] Günter Behr,[2,*] Jiři Málek,[2,3]
Roman Kuzian,[2,4] Stefan-Ludwig Drechsler,[2] Steve Johnston,[2] Alexandre Revcolevschi,[5] Bernd Büchner,[2,6]
Henrik M. Rønnow,[7] Jeroen van den Brink,[2,6] Jochen Geck,[2,†] and Thorsten Schmitt[1,‡]

[1]*Research Department Synchrotron Radiation and Nanotechnology, Paul Scherrer Institut, CH-5232 Villigen PSI, Switzerland*
[2]*Leibniz Institute for Solid State and Materials Research IFW-Dresden, Helmholtzstrasse 20, D-01171 Dresden, Germany*
[3]*Institute of Physics, ASCR, Na Slovance 2, CZ-18221 Praha 8, Czech Republic*
[4]*Donostia International Physics Center (DIPC), ES-20018 Donostia-San Sebastian, Spain*
[5]*Laboratoire de Physico-Chimie de l'Etat Solide, ICMMO, Université Paris-Sud, 91405 Orsay Cedex, France*
[6]*Department of Physics, TU-Dresden, D-01062 Dresden, Germany*
[7]*Laboratory for Quantum Magnetism, ICMP, Ecole Polytechnique Fédérale de Lausanne (EPFL), CH-1015 Lausanne, Switzerland*
(Received 18 October 2012; published 20 February 2013)

We report a high-resolution resonant inelastic soft x-ray scattering study of the quantum magnetic spin-chain materials Li_2CuO_2 and $CuGeO_3$. By tuning the incoming photon energy to the oxygen K edge, a strong excitation around 3.5 eV energy loss is clearly resolved for both materials. Comparing the experimental data to many-body calculations, we identify this excitation as a Zhang-Rice singlet exciton on neighboring CuO_4 plaquettes. We demonstrate that the strong temperature dependence of the inelastic scattering related to this high-energy exciton enables us to probe short-range spin correlations on the 1 meV scale with outstanding sensitivity.

Two-dimensional cuprate materials play an essential role in condensed matter physics as they show high temperature superconductivity upon charge doping. For better understanding these complex materials, it is important to tackle simpler model systems sharing similar key components and showing reduced complexity, namely one dimensional cuprate chains made out of CuO_4 plaquettes. In this context, Zhang-Rice singlets (ZRS) are fundamental elementary excitations being composite objects generic to hole doped or photon excited strongly correlated charge transfer insulators, and that are especially well-known in the cuprates [1]. However, more than two decades after their theoretical discovery and numerous observations afterwards, there is still significant theoretical and experimental activity aimed at clarifying their complex details, e.g., with respect to additional orbitals [2] or specific magnetic correlations beyond their centers [3].

Edge-shared cuprate chains represent a particular class of quantum magnets in which the local geometry gives rise to competing nearest neighbor ferromagnetic (FM) or antiferromagnetic (AFM) exchange coupling J_1 and frustrating next-nearest neighbor AFM J_2 superexchange couplings. The AFM one-dimensional spin-$\frac{1}{2}$ J_1-J_2 Heisenberg model describes such frustrated magnetic interactions, due to which quantum fluctuations can alter both ground state and spin correlations [4]. Generalizing this model by varying the signs and ratio of J_1 and J_2 gives rise to a rich phase diagram with ground states spanning FM, AFM, helical, and gapped singlet states. In real materials, the presence of interchain coupling and occasionally coupling to the lattice

adds complexity to this behavior, rendering theoretical treatment more difficult [5]. It is therefore desirable to obtain experimental access to nearest neighbor spin correlations both within the ground state probed at very low temperature and in thermally occupied excited spin states as a function of temperature (T) [6].

Both Li_2CuO_2 and $CuGeO_3$ realize frustrated edge-shared chain systems that exhibit ground states with completely different intrachain spin correlations. While $CuGeO_3$, on the one hand, displays the well-established spin-Peierls phase below $T_{SP} = 14$ K resulting in a gapped singlet state with pronounced AFM nearest neighbor spin correlations in the chain direction [7,8], Li_2CuO_2, on the other hand, shows FM long-range spin order along the chains below $T_N = 9$ K [9].

In this Letter, we demonstrate that resonant inelastic x-ray scattering (RIXS) at the oxygen K edges allows us to probe ZRS excitations [10,11] for these two quantum magnetic spin-chain materials, Li_2CuO_2 and $CuGeO_3$, with unique sensitivity. Comparing the experimental results to theoretical calculations, we also show that these excitations display an extraordinarily strong temperature dependence, which is directly related to the spin texture of the studied materials. This effect together with the high sensitivity of RIXS is shown to be a powerful probe to study nearest and next nearest neighbor spin correlations in cuprate chains.

RIXS experiments were performed at the ADRESS beam line [12] of the Swiss Light Source, Paul Scherrer Institut, using the SAXES spectrometer [13]. RIXS spectra

were recorded in typically 2 h acquisition time, achieving a statistics of 100–150 photons on the peaks of interest. A scattering angle of 130° was used and all the spectra were measured at the specular position, i.e., at an incidence angle of 65° (see, e.g., Fig. 1 in Ref. [14] for a sketch of the scattering geometry), meaning that no light momentum is transferred to the system along the chain direction. The combined energy resolution was 60 meV at the oxygen K edge (~ 530 eV). Li_2CuO_2 single crystals (which are hygroscopic crystals) [15] were cleaved *in situ* at the pressure of about 5×10^{-10} mbar and at 20 K, while $CuGeO_3$ single crystals were cleaved at 10^{-7} mbar and RT, producing mirrorlike surfaces on both. In the case of Li_2CuO_2, the surface is perpendicular to the [101] axis, so that the CuO_4 plaquettes are tilted 21° away from the surface. In $CuGeO_3$ [16], the surface is oriented perpendicular to the [100] axis, so that the CuO_4 plaquettes are tilted 56° away from the surface.

RIXS probes low-energy charge, spin, orbital, and lattice excitations of solids [17–19]. The RIXS process is based on the coherent absorption and reemission of photons. The incoming photon with energy $\hbar\omega_i$ virtually excites the electronic system from an initial state $|i\rangle$ to an intermediate state $|m\rangle$, which then decays again into a final state $|f\rangle$ by emitting an outgoing photon with energy $\hbar\omega_f$ [17]. We tuned $\hbar\omega_i$ to the oxygen K preedge, as shown by full triangles on the x-ray absorption spectra (XAS) in Figs. 1(a) and 1(b). At this energy, O $1s$ core electrons are directly excited into the upper Hubbard band (UHB) [20,21], which yields a strong resonant enhancement of electronic excitations involving hybridized Cu $3d$ and O $2p$ valence states. Choosing different incident energies corresponds to exciting different intermediate states in the RIXS process.

In Figs. 1(c) and 1(d), RIXS intensities for Li_2CuO_2 and $CuGeO_3$ are plotted as a function of the photon-energy loss $\hbar\Omega = \hbar(\omega_i - \omega_f)$. The unprecedented energy resolution of these data reveals remarkably rich spectra, exhibiting different sharp peaks. For both materials intense and broad structures are observed at $\hbar\Omega > 4.5$ eV that shift with $\hbar\omega_i$ and can be identified as conventional x-ray fluorescence [22]. These transitions will not be considered in the following. Instead, we will focus on the excitations observed at $\hbar\Omega < 4.5$ eV. These excitations occur at fixed energy losses and have the largest intensity when $\hbar\omega_i$ is tuned to the UHB prepeak of the oxygen K edge.

In agreement with previous RIXS studies [23,24] and *ab initio* quantum chemical calculations [25], we assign the sharp peaks at about $\hbar\Omega = 2$ eV in Li_2CuO_2 and 1.9 eV in $CuGeO_3$ to onsite dd excitations, where the hole, which occupies the $3d_{x^2-y^2}$ orbital in the ground state, is excited to a different $3d$ level.

In addition to this, well-resolved excitations are observed at resonance in between the dd excitations and the fluorescence for both Li_2CuO_2 ($\hbar\Omega = 3.2$ eV) and $CuGeO_3$ ($\hbar\Omega = 3.8$ eV), as indicated by arrows in

Figs. 1(c) and 1(d). These two modes are essential for our further analysis. In the case of $CuGeO_3$, this excitation was observed previously and is known to be a ZRS exciton [26–28]. Figure 2 illustrates how such an exciton is created in the RIXS process at the oxygen K edge. Starting from two neighboring CuO_4 plaquettes (d^9, d^9), the system reaches an intermediate state (d^9, $\underline{1s}d^{10}$) after absorbing the incoming photon tuned at the $1s \rightarrow 2p$ resonance of oxygen. In the final step, the $\underline{1s}$ oxygen core hole is filled by a ligand electron from the left plaquette, which results in a ZRS $d^9\underline{L}$ on this plaquette [1] and a d^{10} state on the right plaquette. The extra hole on the left plaquette and the extra electron on the right plaquette form a ZRS exciton. The total spin during this process is conserved at the oxygen K edge. Figure 2 illustrates also that the RIXS intensity of this ZRS exciton will strongly depend on the orientation of the spins on neighboring CuO_4 plaquettes.

As we will show in the following, the 3.2 eV excitation of Li_2CuO_2 also corresponds to a ZRS exciton. In Li_2CuO_2, the situation is more controversial, because in
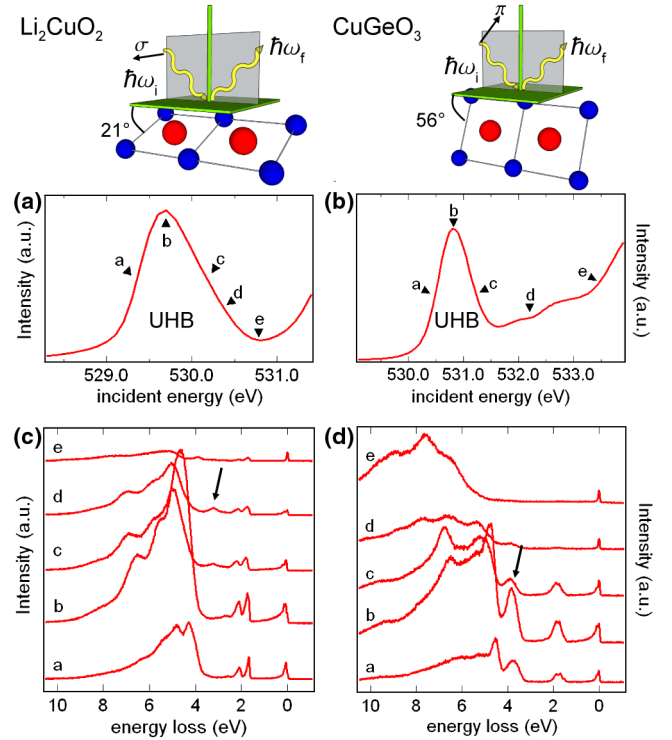

FIG. 1 (color online). Experimental geometry for (left) Li_2CuO_2 and (right) $CuGeO_3$. (a) XAS measured at the oxygen K edge for Li_2CuO_2 with σ-polarized light at 20 K and (b) for $CuGeO_3$ measured with π-polarized light at 40 K (using the total fluorescence yield). Preedge peaks are related to the upper Hubbard band. (c) RIXS spectra (on an energy loss scale) measured at the oxygen K edge for Li_2CuO_2 with σ polarization at 20 K and (d) for $CuGeO_3$ with π polarization at 40 K. The incident energies used for the different spectra are indicated by full triangles on the corresponding XAS spectra in graphs (a) and (b). The RIXS spectra are normalized to the acquisition time.
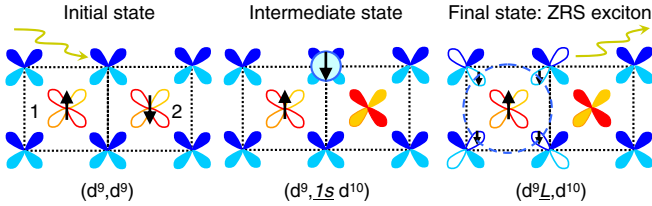
FIG. 2 (color online). Schematic illustration of how a ZRS exciton is created in the RIXS process at the oxygen K edge. See text for detailed explanations. Unoccupied states are depicted with empty orbitals.

previous experiments with RIXS [23] and other experimental techniques [29–31], the ZRS exciton could not be unambiguously observed.

The most striking characteristic in the RIXS data is the dramatic T dependence of the spectral peaks at about 3.5 eV, which is present in both materials, see Fig. 3. Interestingly, in Li_2CuO_2 the exciton intensity increases with temperature whereas in $CuGeO_3$ it follows the opposite behavior [see Figs. 3(a) and 3(b)]. These temperature dependences imply that high energy excitations at about 3.5 eV are strongly affected by thermal fluctuations corresponding to an energy scale of merely $k_B T \sim 1$ meV. We will show that these high-energy modes directly reflect the character of nearest neighbor spin correlations (see Fig. 2), as the probability for a ZRS to be excited in RIXS strongly depends on the relative orientation of neighboring copper spins. In order to obtain a more detailed microscopic understanding of the nature of this strong temperature dependence, we performed many-body cluster calculations based on a pd Hamiltonian for three up to five CuO_4 plaquettes (trimers, tetramers, and pentamers) [10,32–34] (see Ref. [35] for more details). The use of a small cluster is justified by the fact that the electronic system of the edge-shared cuprates is well localized.
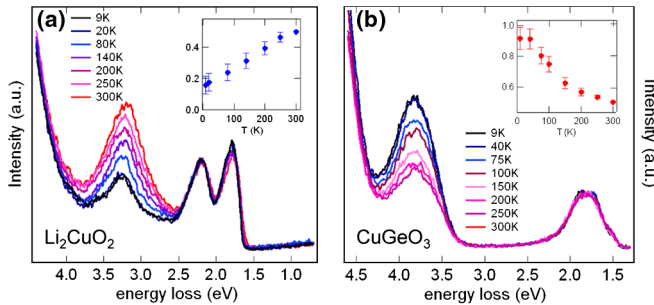
We illustrate the underlying physics with the trimer results for the sake of simplicity. Analogous results have been obtained on tetramers (not shown in this work) and pentamers (as shown in Fig. S3 of the Supplemental Material [35]). The trimer has eigenstates $|i, S_i\rangle$ with total spin $S_i = \frac{1}{2}$ and $S_i = \frac{3}{2}$, corresponding to the spin configurations ↑↓↑ (AFM) and ↑↑↑ (FM), respectively. At finite temperature T, not only the ground state, but also all eigenstates $|i, S_i\rangle$ within an energy range $\sim k_B T$ will be populated. This includes states with different S_i and corresponds to thermal spin fluctuations. For both Li_2CuO_2 and $CuGeO_3$ three $|i, S_i\rangle$ were found to be significantly populated within the studied temperature range [see Ref. [35] and Figs. 4(a) and 4(b)]: two doublets with $S_i = \frac{1}{2}$ ($D_{1,2}$), differing from each other in charge distribution among hybridized p and d states, and one quadruplet with $S_i = \frac{3}{2}$ (Q_1). However, their energy sequence is reversed for the two systems.

Each of the thermally populated $|i, S_i\rangle$ acts as an initial state for RIXS and opens specific excitation channels $|i, S_i\rangle \rightarrow |f, S_f\rangle$. Hence, every populated $|i, S_i\rangle$ contributes with a partial intensity $\mathcal{I}_i$, properly weighted in the total RIXS signal $I(T)$ at a specific temperature T as explained in Refs. [10,35].

The calculated $\mathcal{I}_i$ for Li_2CuO_2 and $CuGeO_3$ are presented in Figs. 4(a) and 4(b) respectively. It can be seen that the $\mathcal{I}_i$ originating from D_1, D_2, and Q_1 are all distinctly different and, moreover, that a low energy charge transfer excitation exists, which can only be reached from $D_{1,2}$. The calculations identify this excitation as the ZRS exciton $(d^9, d^9) \rightarrow (d^{10}, d^9\underline{L})$ as illustrated in Fig. 2.
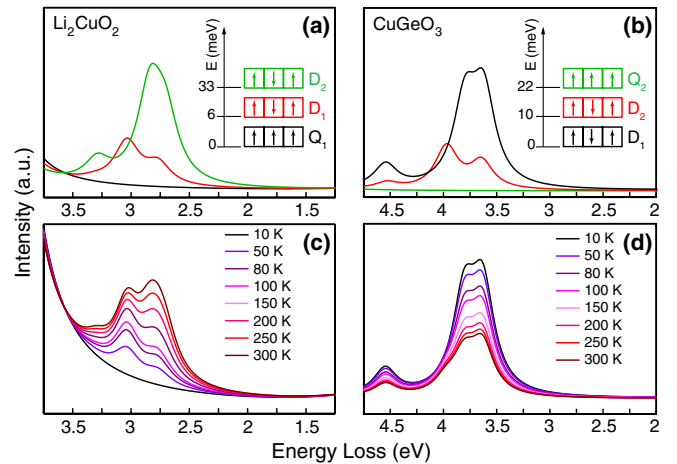

FIG. 3 (color online). (a) Temperature dependent RIXS data for Li_2CuO_2 measured with σ polarization and an excitation energy of 530.1 eV and (b) for $CuGeO_3$ measured with π polarization and an excitation energy of 530.8 eV. The spectra are plotted in an energy loss scale. The spectra have been normalized to the area of the dd excitations (see Supplemental Material [35]). The integrated intensity of the ZRS peaks as a function of temperature is displayed in the corresponding insets.

FIG. 4 (color online). (a) Partial RIXS intensity $\mathcal{I}_i$ calculated from the ground state (black line) of a Cu_3O_8 cluster and the two excited states (red and green lines), respectively, for Li_2CuO_2 and (b) for $CuGeO_3$. Using the same color code, a schematic representation of the eigenstates and corresponding eigenenergies is shown. (c), Total RIXS signal $I(T)$ as a function of temperature for Li_2CuO_2 and (d) $CuGeO_3$ (Fig. S3 of the Supplemental Material shows analogous results for a Cu_5O_{12} cluster for comparison).

The fact that the ZRS exciton can only be reached from the initial states $D_{1,2}$ and not from Q_1, is a direct consequence of the conservation of spin ($S_f = S_i$) in oxygen K edge RIXS. Such selection rules explain the strong T dependence of the ZRS exciton intensity as shown in Figs. 4(c) and 4(d), which is given by the thermal population of the excited multiplet D states in the case of Li_2CuO_2.

Both the excitation energies and the T dependence of the ZRS exciton obtained in the model calculations for Li_2CuO_2 [Fig. 4(c)] and $CuGeO_3$ [Fig. 4(d)] agree very well with the T-dependent peak found in our experiment [Figs. 3(a) and 3(b)]. This unambiguously identifies the experimentally observed excitations at 3.2 eV in Li_2CuO_2 and at 3.8 eV in $CuGeO_3$ as ZRS excitons. Our calculated RIXS spectra [Figs. 4(c) and 4(d)] do not reproduce the exact energy positions of the ZRS peaks of the experimental spectra [Figs. 3(a) and 3(b)]. These slight discrepancies come from the relative simplicity of our model Hamiltonian as well as the chosen boundary conditions (see Supplemental Material for a more detailed discussion [35]). However, this does not affect the calculated qualitative features of the ZRS exciton, which are robust and which are the main focus of the present study.

The fact that creating a ZRS exciton depends on the probability of two neighboring spins being antiparallel has an important consequence: it enables us to study intrachain nearest neighbor spin correlations by oxygen K edge RIXS. In $CuGeO_3$, for instance, spins along the chain are antiparallel in the ground state. Upon decreasing T, thermally driven fluctuations out of this ground state decrease, yielding a higher intensity of the corresponding ZRS exciton. Vice versa, if the spins along the chain are parallel in the ground state, the ZRS exciton peak becomes weaker upon cooling.

The results in Fig. 3(a) not only resolve the issue of the ZRS exciton assignment in Li_2CuO_2, but also verify that the spins within chains in Li_2CuO_2 are FM ordered at low temperatures. Another important observation for Li_2CuO_2 is that even at 9 K the ZRS exciton peak does not disappear, but retains a significant intensity [see Fig. 3(a)] in agreement with the weaker structure of the low-T spectrum calculated for pentamers (see our Fig. S3 in Ref. [35]). This spectral structure is fully lacking for trimers as shown in Fig. 4(c). This is due to the fact that the first excited state in the trimer is at 6.0 meV, whereas for the larger pentamer it is lowered to only 1.1 meV (which corresponds to about 13 K). The comparison between theory and experiment therefore shows that for a realistic estimate of the excitation energies larger clusters like the pentamer have to be considered.

Both the experimental and theoretical results point to sizable residual quantum and thermal fluctuations out of the intrachain FM ground state. The present data indicate that these fluctuations in Li_2CuO_2 persist down to low temperatures and that this system may be very close to the quantum critical point, which separates FM from helical (AFM) intrachain order. This observation agrees very well with a previous neutron study, where the proximity to a quantum critical point was inferred from an analysis of the magnon dispersion [9], whereas in the present case we observe the thermal and quantum nearest neighbor spin correlations directly. We note that a quantitative modeling of the RIXS spectra as a function of temperature will require consideration of interchain interactions, domain walls, and also impurities, which can also contribute to the residual spectral weight in the ZRS exciton. This, however, is well beyond the scope of the present study.

Following Ref. [10], we remind the reader that the Zeeman splitting of the nonsinglet excited states caused by an external magnetic field affects their thermal population. In the perspective of our present work, this suggests that RIXS measurements in magnetic fields might be helpful to resolve the nature of the involved spin states.

In conclusion, we have performed RIXS measurements at the oxygen K edge on the edge-sharing chain compounds, Li_2CuO_2 and $CuGeO_3$. Supported by calculations within the five-band extended Cu $3d$ O $2p$ Hubbard model, we have shown that our temperature dependent measurements give access to the nearest neighbor spin correlations of these materials. This is brought about via the entanglement of spin, orbital, and charge degrees of freedom that characterizes strongly correlated, magnetically frustrated materials. RIXS at the oxygen K edge can therefore be used as a versatile and powerful photon-in–photon-out method to investigate the low-energy magnetic short-range spin fluctuations in large gap charge transfer insulators with great sensitivity.

*Deceased.
†j.geck@ifw-dresden.de
‡thorsten.schmitt@psi.ch

[1] F. C. Zhang and T. M. Rice, Phys. Rev. B **37**, 3759 (1988).

[2] C.-C. Chen, B. Moritz, F. Vernay, J. N. Hancock, S. Johnston, C. J. Jia, G. Chabot-Couture, M. Greven, I. Elfimov, G. A. Sawatzky, and T. P. Devereaux, Phys. Rev. Lett. **105**, 177401 (2010).

[3] T. Morinari, J. Phys. Soc. Jpn. **81**, 074716 (2012).

[4] H.-J. Mikeska and A. K. Kolezhuk, Lect. Notes Phys. **645**, 1 (2004).

[5] R. Zinke, S.-L. Drechsler, and J. Richter, Phys. Rev. B **79**, 094425 (2009).

[6] N. N. Kovaleva, A. V. Boris, C. Bernhard, A. Kulakov, A. Pimenov, A. M. Balbashov, G. Khaliullin, and B. Keimer, Phys. Rev. Lett. **93**, 147204 (2004).

[7] M. Hase, I. Terasaki, and K. Uchinokura, Phys. Rev. Lett. **70**, 3651 (1993).

[8] G. Castilla, S. Chakravarty, and V. J. Emery, Phys. Rev. Lett. **75**, 1823 (1995).

[9] W. E. A. Lorenz, R. O. Kuzian, S.-L. Drechsler, W.-D. Stein, N. Wizent, G. Behr, J. Málek, U. Nitzsche, H. Rosner, A. Hiess, W. Schmidt, R. Klingeler, M. Loewenhaupt, and B. Büchner, Europhys. Lett. **88**, 37002 (2009).

[10] J. Málek, S.-L. Drechsler, U. Nitzsche, H. Rosner, and H. Eschrig, Phys. Rev. B **78**, 060508(R) (2008).

[11] Y. Matiks, P. Horsch, R. K. Kremer, B. Keimer, and A. V. Boris, Phys. Rev. Lett. **103**, 187401 (2009).

[12] V. N. Strocov, T. Schmitt, U. Flechsig, T. Schmidt, A. Imhof, Q. Chen, J. Raabe, R. Betemps, D. Zimoch, J. Krempasky, X. Wang, M. Grioni, A. Piazzalunga, and L. Patthey, J. Synchrotron Radiat. **17**, 631 (2010).

[13] G. Ghiringhelli, A. Piazzalunga, C. Dallera, G. Trezzi, L. Braicovich, T. Schmitt, V. N. Strocov, R. Betemps, L. Patthey, X. Wang, and M. Grioni, Rev. Sci. Instrum. **77**, 113108 (2006).

[14] L. Braicovich, M. Moretti Sala, L. J. P. Ament, V. Bisogni, M. Minola, G. Balestrino, D. Di Castro, G. M. De Luca, M. Salluzzo, G. Ghiringhelli, and J. van den Brink, Phys. Rev. B **81**, 174533 (2010).

[15] N. Wizent, G. Behr, W. Löser, B. Büchner, and R. Klingeler, J. Cryst. Growth **318**, 995 (2011).

[16] G. Dhalenne, A. Revcolevschi, J. C. Rouchaud, and M. Fedoroff, Mater. Res. Bull. **32**, 939 (1997).

[17] L. J. P. Ament, M. van Veenendaal, T. P. Devereaux, J. P. Hill, and J. van den Brink, Rev. Mod. Phys. **83**, 705 (2011).

[18] J. Schlappa, K. Wohlfeld, K. J. Zhou, M. Mourigal, M. W. Haverkort, V. N. Strocov, L. Hozoi, C. Monney, S. Nishimoto, S. Singh, A. Revcolevschi, J.-S. Caux, L. Patthey, H. M. Ronnow, J. van den Brink, and T. Schmitt, Nature (London) **485**, 82 (2012).

[19] J. Schlappa, T. Schmitt, F. Vernay, V. N. Strocov, V. Ilakovac, B. Thielemann, H. M. Ronnow, S. Vanishri, A. Piazzalunga, X. Wang, L. Braicovich, G. Ghiringhelli, C. Marin, J. Mesot, B. Delley, and L. Patthey, Phys. Rev. Lett. **103**, 047401 (2009).

[20] R. Neudert, H. Rosner, S.-L. Drechsler, M. Kielwein, M. Sing, Z. Hu, M. Knupfer, M. S. Golden, J. Fink, N. Nucker, M. Merz, S. Schuppler, N. Motoyama, H. Eisaki, S. Uchida, M. Domke, and G. Kaindl, Phys. Rev. B **60**, 13 413 (1999).

[21] V. Corradini, A. Goldoni, F. Parmigiani, C. Kim, A. Revocolevschi, L. Sangaletti, and U. del Pennino, Surf. Sci. **420**, 142 (1999).

[22] A. Kotani and S. Shin, Rev. Mod. Phys. **73**, 203 (2001).

[23] T. Learmonth, C. McGuinness, P.-A. Glans, J. E. Downes, T. Schmitt, L.-C. Duda, J.-H. Guo, F. C. Chou, and K. E. Smith, Europhys. Lett. **79**, 47012 (2007).

[24] L.-C. Duda, J. E. Downes, C. McGuinness, T. Schmitt, A. Augustsson, K. E. Smith, G. Dhalenne, and A. Revcolevschi, Phys. Rev. B **61**, 4186 (2000).

[25] H.-Y. Huang, N. A. Bogdanov, L. Siurakshina, P. Fulde, J. van den Brink, and L. Hozoi, Phys. Rev. B **84**, 235125 (2011).

[26] F. Bondino, M. Zangrando, M. Zacchigna, G. Dhalenne, A. Revcolevschi, and F. Parmigiani, Phys. Rev. B **75**, 195106 (2007).

[27] S. Atzkern, M. Knupfer, M. S. Golden, J. Fink, A. Hubsch, C. Waidacher, K. W. Becker, W. von der Linden, M. Weiden, and C. Geibel, Phys. Rev. B **64**, 075112 (2001).

[28] J. Kim, D. S. Ellis, H. Zhang, Y.-J. Kim, J. P. Hill, F. C. Chou, T. Gog, and D. Casa, Phys. Rev. B **79**, 094525 (2009).

[29] S. Atzkern, M. Knupfer, M. S. Golden, J. Fink, C. Waidacher, J. Richter, K. W. Becker, N. Motoyama, H. Eisaki, and S. Uchida, Phys. Rev. B **62**, 7845 (2000).

[30] Y. Mizuno, T. Tohyama, S Maekawa, T. Osafune, N. Motoyama, H. Eisaki, and S. Uchida, Phys. Rev. B **57**, 5326 (1998).

[31] Y.-J. Kim, J. P. Hill, F. C. Chou, D. Casa, T. Gog, and C. T. Venkataraman, Phys. Rev. B **69**, 155105 (2004).

[32] K. Okada and A. Kotani, Phys. Rev. B **65**, 144530 (2002).

[33] K. Okada and A. Kotani, J. Phys. Soc. Jpn. **76**, 123706 (2007).

[34] K. Okada and A. Kotani, Phys. Rev. B **63**, 045103 (2001).

[35] See Supplemental Material at http://link.aps.org/supplemental/10.1103/PhysRevLett.110.087403 for a detailed description of our theoretical model.